

Implementation of a drive-by monitoring system for transport infrastructure utilising smartphone technology and GNSS

P. J. McGetrick¹ · D. Hester¹ · S. E. Taylor¹

Received: 31 October 2016 / Accepted: 28 February 2017 / Published online: 10 March 2017
© The Author(s) 2017. This article is published with open access at Springerlink.com

Abstract Ageing and deterioration of infrastructure are a challenge facing transport authorities. In particular, there is a need for increased bridge monitoring in order to provide adequate maintenance, prioritise allocation of funds and guarantee acceptable levels of transport safety. Existing bridge structural health monitoring (SHM) techniques typically involve direct instrumentation of the bridge with sensors and equipment for the measurement of properties such as frequencies of vibration. These techniques are important as they can indicate the deterioration of the bridge condition. However, they can be labour intensive and expensive due to the requirement for on-site installations. In recent years, alternative low-cost indirect vibration-based SHM approaches have been proposed which utilise the dynamic response of a vehicle to carry out ‘drive-by’ pavement and/or bridge monitoring. The vehicle is fitted with sensors on its axles thus reducing the need for on-site installations. This paper investigates the use of low-cost sensors incorporating global navigation satellite systems (GNSS) for implementation of the drive-by system in practice, via field trials with an instrumented vehicle. The potential of smartphone technology to be harnessed for drive-by monitoring is established, while smartphone GNSS tracking applications are found to compare favourably in terms of accuracy, cost and ease of use to professional GNSS devices.

Keywords Acceleration · Drive-by bridge monitoring · Global navigation satellite systems · Structural health monitoring · Vehicle sensors

1 Introduction

Bridges and pavements form an integral part of transport infrastructure worldwide. Over their lifetime, their condition will deteriorate due to factors such as environmental conditions, ageing and increased traffic loading. In countries such as the USA, Korea, Japan and across the EU, a majority of bridge structures are now over 50 years old [1, 2]. This leads to the requirement for increased monitoring and maintenance in order to prioritise allocation of funds and guarantee acceptable levels of transport safety, particularly where rehabilitation and life extension of bridge structures are necessary.

As traditional visual inspection methods for bridges can be highly variable, relying on visible signs of deterioration, bridge management systems (BMSs) are now more commonly integrating structural health monitoring (SHM) methods, involving direct instrumentation of bridge structures with sensors and data acquisition equipment, which target identification of damage from dynamic structural responses [3, 4]. However, these methods can be labour intensive and expensive due to the requirement for on-site installations, which may require dense sensor networks. This has restricted widespread implementation of SHM for short and medium-span bridges, which form the greatest proportion of bridges in service. Therefore, a more efficient alternative is required which can provide information about a bridge’s condition.

Road pavement profile measurements are typically obtained using an inertial profilometer, which consists of a

✉ P. J. McGetrick
p.mcgetrick@qub.ac.uk

¹ School of Natural and Built Environment, David Keir Building, Queen’s University Belfast, Belfast BT9 5AG, Northern Ireland, UK

vehicle equipped with a height sensing device, such as a laser, which measures pavement elevations at regular intervals [5] with the effects of vehicle dynamics removed from the elevation measurements via accelerometer(s) and gyroscopes. The vehicle can travel at highway speeds and the method provides accurate, high-resolution profile measurements but a drawback is the expense associated with laser-based technology.

In recent years, alternative low-cost indirect vibration-based SHM approaches have been proposed by a number of researchers which utilise the dynamic response of a vehicle to carry out ‘drive-by’ monitoring of bridges [6, 7] and/or pavements [8]. The vehicle is fitted with sensors, such as accelerometers, on its axles to monitor vibration thus aiming to reduce the need for (a) on-site SHM installations on the bridge which can be expensive and (b) expensive laser-based technology and sensors currently used in inertial road profilometers. Methods have been proposed and developed which target identification of bridge dynamic properties such as frequency [9, 10], damping [11], mode shapes [12] and modal curvatures [13] based on post-processing of on-vehicle sensor measurements, showing some promise. However, these types of methods, summarised by Malekjafarian et al. [7], lack comprehensive experimental verification, with very few field trials reported in the literature. Those reporting successful results have been primarily limited to bridge frequency identification, such as the experiments by Lin and Yang [6] utilising a truck-trailer configuration, or the light commercial vehicle employed by both Siringoringo and Fujino [14] and Fujino et al. [15]. In general, speeds below 40 km/h have been found to provide the most accurate bridge frequency identification results due to improved spectral resolution and the reduced influence of road profile on the vehicle response, while modal analysis of the test vehicle is recommended before field testing commences. Based on existing research [7], three main challenges for drive-by monitoring have been identified as the road profile, the limited vehicle-bridge interaction (VBI) time (speed-dependent) and environmental effects, while also acknowledging practical issues such as ongoing traffic on a bridge and variation in speed of the instrumented vehicle.

Malekjafarian et al. [7] suggest that a potential solution to challenges related to limited VBI time and environmental effects is the use of instrumented vehicles that repeatedly pass over the same bridge, or pavement, potentially at different speeds less than 40 km/h. This solution is effectively a long-term monitoring approach. It could be implemented by instrumenting a fleet of vehicles with sensors, e.g. public vehicles such as the public bus monitoring system investigated in Japan by Miyamoto and Yabe [16], which drive along the same route multiple times per day. This system [16] utilises conventional sensors and

data acquisition electronics while two operators are required to record test conditions such as bridge entry/exit, number of bus occupants, bus speed and number of oncoming vehicles. An alternative lower-cost possibility is proposed in this paper; the use of smartphone technology and sensors requires only one operator, i.e. the driver. Due to the current prevalence of such technology, drive-by monitoring systems could potentially move beyond the limitation to unique instrumented vehicles, or localised instrumented vehicle fleets.

This paper is motivated by the aforementioned lack of field testing and thus investigates the implementation of such drive-by monitoring systems in practice via field trials. For this purpose, a two-axle vehicle is instrumented with accelerometers and global navigation satellite system (GNSS) receivers and is driven along predetermined routes in the Belfast road network. Aiming to take advantage of existing low-cost technologies, in addition to accelerometers designed for structural applications and a Leica GNSS receiver, smartphone accelerometers and global position tracking applications are also utilised during field trials. Measurements obtained from all sensors and receivers are compared in terms of accuracy, system cost and ease of use. Identification of pavement features, bridge expansion joints and bridge frequency from vehicle acceleration measurements are investigated in order to evaluate the feasibility of this low-cost monitoring system in practice.

2 Methodology

For this field investigation, the instrumented vehicle was a Ford Transit van (Fig. 1), weighing 1600 kg and fitted with accelerometers to measure vibration and GNSS receivers to record the vehicle position in the road network. A digital camera was also used to record video footage of each vehicle test run while the average vehicle speed during



Fig. 1 Instrumented vehicle

testing was 23 mph (36 km/h). The details of instrumentation and setup are outlined in the following sections.

2.1 Acceleration measurement setup

The overall setup of accelerometers in the vehicle is illustrated in Fig. 2, consisting of 4 accelerometers measuring vertical vibration.

2.1.1 Wired accelerometers

Two wired uniaxial accelerometers were installed at the same location in the body of the vehicle, adhesively mounted over the left rear wheel. This location was selected based on findings of past experimental studies carried out by the authors, in which sensors mounted in the body of the vehicle over a lighter axle proved more sensitive to external excitation of the vehicle [17]. In addition, it also enabled easy access for instrumentation purposes. The installed accelerometers were ultra-low noise signal conditioned model 4610A-002 (± 2 g) and 4610A-005 (± 5 g) units by Measurement SpecialtiesTM, shown in Fig. 2b, which provide low-pass filtered output over a DC–300 Hz bandwidth. Excitation voltage was provided by a 9-V battery during testing. Both ± 2 and ± 5 g rated accelerometers were tested for comparison with smartphone sensors and to ensure any large magnitude vehicle accelerations greater than 2 g were recorded. The sampling frequency was 1000 Hz allowing potential identification of any features with frequency components between 100 Hz and 500 Hz, which would be undetected by the smartphone sensors. However, no such features were identified.

2.1.2 Smartphone sensors

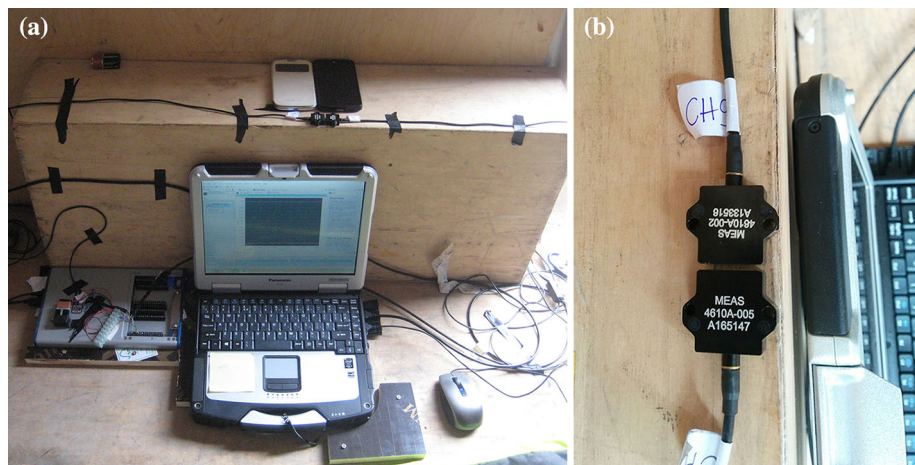
The built in accelerometers of an LG Nexus 5 and a Samsung Galaxy S4 were used for vertical smartphone

acceleration measurements; both devices were mounted over the left rear wheel with adhesive (Fig. 2a). The LG Nexus 5, retailing at €290 approximately as of summer 2016, contains a 6-axis MPU-6515 chip with integrated triaxial MEMS Gyroscope and triaxial MEMS accelerometer by InvenSense Inc., built into the device motherboard. The maximum measurement range during testing was ± 19.61 m/s², equivalent to ± 2 g, although this can be increased. As vehicle body and bridge vibration magnitudes are generally less than 2 g, this range is suitable for bridge monitoring applications. The smartphone sampling frequency was set at a maximum of 200 Hz, which is also adequate for drive-by monitoring.

The Samsung S4, retailing at €220 approximately as of summer 2016, uses a K330 triaxial accelerometer by STMicroelectronics. Similar to the Nexus 5, the maximum measurement range was ± 19.61 m/s² (± 2 g); however, the maximum allowable sampling frequency on the Samsung S4 was 100 Hz during testing. In practice, 100 Hz is suitable for drive-by monitoring methods as the vehicle and bridge modes of vibration which are of interest in measured dynamic responses generally have frequencies less than the associated Nyquist frequency of 50 Hz. Nevertheless, a higher sampling frequency as provided by the Nexus 5 (200 Hz) and the wired accelerometer setup (1000 Hz) can be desirable to ensure any potential aliasing is avoided in the signal response, depending on the drive-by application.

Accelerations were logged to the internal SD card of each device via the Android smartphone application ‘Vibration Alarm’ by Mobile Tools, freely available via the Google Play Store. This application ran in the background during testing. In terms of sampling consistency, it was observed that that for around 3% of the total number of recorded samples, the sample interval varied by ± 0.001 s for both devices. This resulted in sample intervals of 0.005 ± 0.001 s for the Nexus 5, and 0.01 ± 0.001 s for the Samsung S4, respectively. Measured data were therefore

Fig. 2 a Accelerometer instrumentation setup, b uniaxial accelerometers



interpolated to overcome this and obtain a consistent sampling interval.

Each accelerometer was powered by the internal lithium-ion batteries of their respective smartphones; the Nexus 5 by a 3.8 V, 2300 mAh battery and the S4 by a 3.8 V, 2600 mAh battery. An external 5200 mAh capacity portable power supply (cost of €16) was also used as backup for the LG Nexus 5. For similar applications in a vehicle fleet, a power adaptor with USB output connected to the 12 V source output of the vehicle could be used as an alternative.

2.2 GNSS setup

In addition to recording acceleration measurements, accurately monitoring the position of the instrumented vehicle during its passage along a road network is valuable for a number of reasons. Firstly, if anomalous results or large peaks are observed in the acceleration record, they can be tagged with a location via GNSS tracking, allowing the engineer to rapidly pinpoint areas with potential pavement damage, e.g. potholes or cracking. This type of approach has already been investigated for pothole detection in pavements using custom built devices combining accelerometers and GPS receivers [18], further incorporating video to enable screenshots of areas of interest [19], and smartphone applications integrating crowdsourcing [20], that primarily rely on acceleration peak magnitudes which exceed a particular threshold being recorded by smartphones in multiple vehicles at a particular location. Secondly, for bridge monitoring, it would enable approximate identification of bridge crossings by the vehicle, allowing specific portions of the acceleration signal to be extracted and analysed using one of the many methods proposed in the literature [7]. In this paper, recorded GNSS tracks are used to identify pavement sections and a bridge crossing of interest, for which the corresponding signal is extracted and processed using a fast Fourier transform for the purposes of bridge frequency identification. Therefore, this analysis aims not only to identify possible potholes or deterioration via acceleration peaks, but also to identify dynamic properties of the bridge.

2.2.1 Leica GNSS smart antenna

To serve as a reference for the vehicle position recorded by the Nexus 5 smartphone during testing, a survey-grade Leica Geosystems Viva GS14 GNSS smart rover antenna was used to log the vehicle location coordinates to a removable SD card throughout testing, incorporating Network Real-Time Kinematic (RTK) corrections [21] obtained via the local mobile network. The antenna was mounted magnetically on the roof of the van and operated

using a Leica Geosystems CS15 controller (see Fig. 3). Positioning errors with this system are ± 8 mm (horizontal) and ± 15 mm (vertical), respectively, for static measurements, although this is dependent upon various factors such as the number of satellites tracked, constellation geometry and observation time. Positioning error was expected to vary during testing, particularly in urban or wooded areas where satellite visibility or signal strength can be restricted, and due to the movement of the vehicle.

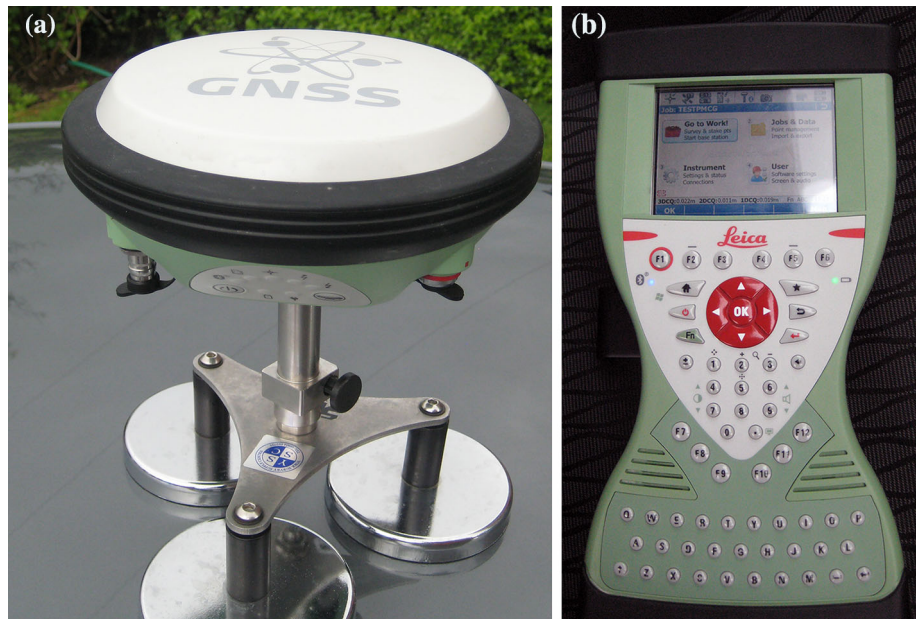
2.2.2 Smartphone application

The vehicle location was also tracked during testing using a freely available Android smartphone application installed on the LG Nexus 5, namely ‘GPSEssentials’ by Schollmeyer [22]. This particular application was selected as it allows the vehicle coordinates to be recorded and time-stamped every second and can plot the resulting tracks in real time, or export them in.kml format for viewing on Google Earth. It also can provide a range of other outputs such as average speed and elevation. This application utilises the smartphone’s GNSS transceiver (a Qualcomm WTR1605L) which supports Assisted-GPS (A-GPS) and GLONASS constellations. A-GPS techniques enable smartphone receivers to achieve positioning in indoor locations and urban canyons formed by buildings, similar to routes travelled along in this investigation. An investigation by Zandbergen and Barbeau [23] showed that median horizontal positioning errors of such systems can fall between 5 and 8.5 m. In a recent detailed vehicle tracking performance evaluation, Gikas and Perakis [24] conclude that modern smartphones can provide very good navigation solutions for a wide range of road applications due to embedded GNSS, Inertial Measurement Unit (IMU) sensors and similar devices. However, in their field investigation they observed that smartphone positioning performance varies depending on filtering approaches used by different manufacturers and it degraded approximately by a factor of two when satellite signals were obstructed, e.g. by buildings or trees. In addition, for open sky conditions the mean along-track errors (4.83–8.56 m) were found to be higher than the mean off-track errors (1.4–3.29 m) for the smartphones, indicating that a vehicle’s lane, or transverse position on the road, can be more accurately identified than a crossing over a bridge.

2.3 Data acquisition

A National Instruments (NI) multifunction USB-6353 X-Series data acquisition (DAQ) device was used to log wired accelerometer measurements to a Panasonic Toughbook running NI Signal Express. The analogue-to-digital converter had a resolution of 16 bits. During testing,

Fig. 3 **a** Leica GS14 smart antenna, **b** Leica CS15 controller



power to the DAQ device was provided by a 12 V car battery placed in the rear of the vehicle, with the required output of 230Vac provided by an inverter (Fig. 4). The total cost of this DAQ setup was approximately €7000.

2.4 Test routes

Two test routes in the Belfast region of Northern Ireland were selected for testing, shown marked in Google maps in Fig. 5. Each route passes through urban and wooded areas where clear views of the sky are obstructed, in addition to including bridge crossings. Route 1 was 2.2 miles (3.5 km) long while Route 2 was 12 miles (18 km) but also included repeat bridge crossings over the M1 motorway. Both routes

as tracked using tested GNSS systems are shown in Sect. 3.2.

3 Identification of features

3.1 Acceleration measurements

Figure 6 shows the full time history of raw acceleration measurements obtained from all accelerometers in the instrumented vehicle for route 1 with gravitational acceleration removed, while Fig. 7 shows the corresponding spectra. The power spectrum for the 5 g accelerometer was similar to that for the 2 g accelerometer thus has been omitted. It can be seen from Fig. 6 that despite the differences in sampling frequency, the smartphone acceleration time histories compare relatively well to the corresponding measurements from the wired 2 g accelerometer (Fig. 6b), with peak acceleration occurrences matching.

Figure 6a shows the wired 5 g accelerometer measurements for comparative purposes—any acceleration exceeding the ± 2 g limit of the other sensors was expected to appear in this response, potentially identifying a significant feature. Four peaks are marked in Fig. 6a, b which exceeded +2 g, or in this case $+9.81 \text{ m/s}^2$ due to the removal of gravitational acceleration. Although the maximum peak magnitudes measured by the wired accelerometers were not reached by the smartphones due to their range limits, the Nexus 5 accelerometer reached its range limit more consistently for peaks exceeding 2 g. This suggests that it may be a more suitable device for drive-by



Fig. 4 Power supply for data acquisition device

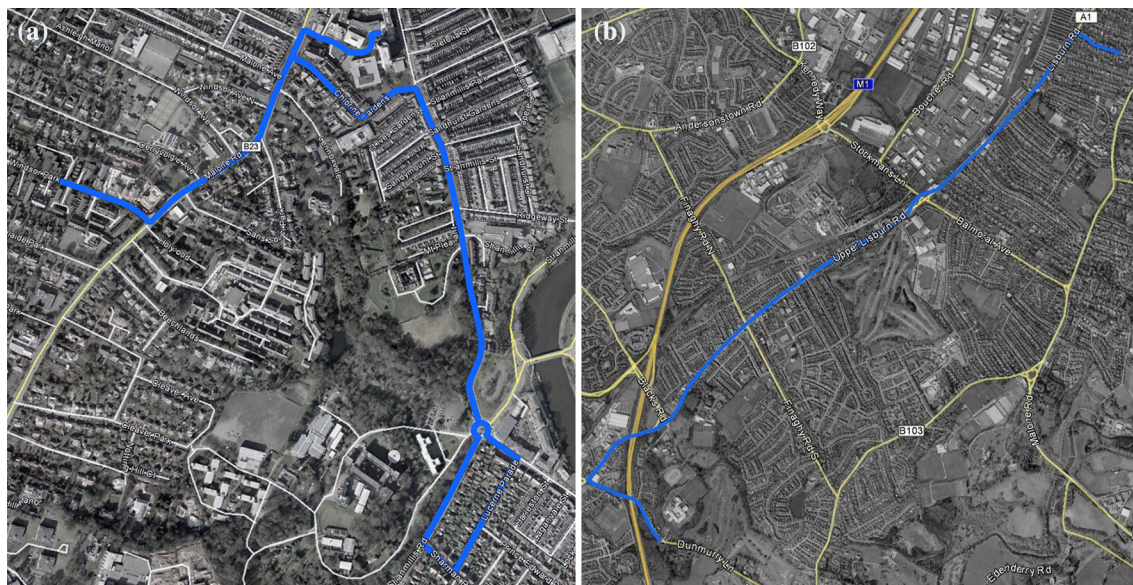


Fig. 5 a Test route 1, b test route 2

monitoring purposes than the Samsung S4, despite registering 2 peaks that did not exceed $+9.81 \text{ m/s}^2$ for the wired accelerometers. Furthermore, the Nexus 5 has the potential to have its accelerometer's dynamic range increased by the user. The Samsung S4 accelerometer (Fig. 6d) is not as sensitive to the overall vibration magnitude as the Nexus 5, in many cases registering less than half the peak acceleration magnitude, which is influenced by its 100 Hz sampling frequency limitation. This is also reflected in the spectra (Fig. 7).

Although the dominant body bounce vibration mode of the vehicle at 2.3 Hz can be observed as a peak in the spectra for all sensors in Fig. 7, the smartphone peak magnitude is approximately 9 times less than that recorded by the wired sensor, indicating lower sensitivity. However, this relative magnitude difference is reflected across the whole frequency spectrum. Further vehicle-related frequencies are identified by all sensors at 14.8 and 25 Hz. A clear peak at 32.5 Hz is also observed in Fig. 7 for the wired accelerometers. This peak corresponds to the idling engine frequencies of the vehicle while it was motionless; a related peak appears in the smartphone responses but is not very significant. The relatively low sensitivity of the smartphone sensors to this frequency can also be observed in the acceleration time history during idling periods, e.g. between 500 and 560 s in Fig. 6. Lastly, a peak also occurs in the acceleration spectra close to 60 Hz for the Nexus 5 smartphone, highlighting sensitivity to electrical noise. The wired uniaxial accelerometers do not suffer from this issue as they have been designed and constructed for applications requiring low levels of output signal noise. Although most frequencies of interest for bridge

monitoring applications will fall well below this, it does raise the overall issue of smartphone sensor suitability in terms of signal quality for drive-by monitoring algorithms. For this reason, further analysis presented in the following section incorporates post-processing of all measured accelerations using a low-pass filter.

3.1.1 Filtered acceleration measurements

Prior to confirming identification of features, all acceleration measurements are filtered using a low-pass digital Butterworth filter with a cut-off frequency of 20 Hz. The filtered acceleration responses corresponding to Fig. 6 are shown in Fig. 8, while the revised spectra are shown in Fig. 9. Figure 8 demonstrates a significant improvement over the raw acceleration time histories; all measurements now show comparable peak and overall magnitude responses following the filtering process. Inspecting these figures manually, an initial threshold of $\pm 6 \text{ m/s}^2$ is used to identify common peaks for further investigation. The magnitudes and occurrence times for all peaks exceeding this threshold are given in Table 1. Where both positive and negative peaks both exceed the threshold at a particular time, only the larger acceleration magnitude is given in the table. Each accelerometer response follows a similar trend. It is clear that Peak 3 causes the largest vehicle response, followed by Peaks 0, 2 and 1, respectively, in order of magnitude. Peaks 4 and 7 give slightly lower responses while peaks 5 and 6 give the lowest responses, with peak 6 not exceeding the threshold for the smartphone accelerometers. The times corresponding to these peaks in the acceleration signals (numbered chronologically) are

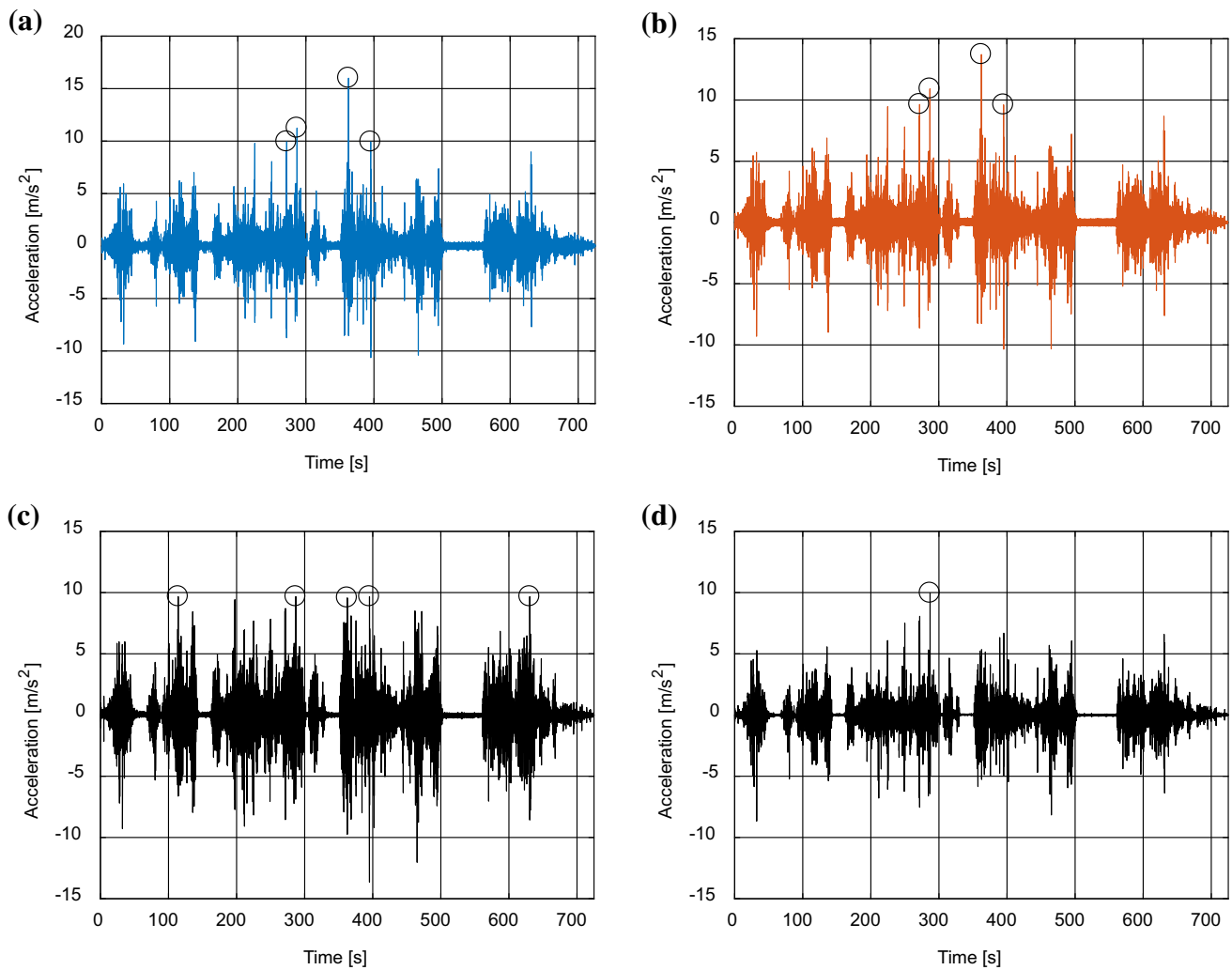


Fig. 6 Original acceleration measurements for test route 1 **a** 5 g uniaxial, **b** 2 g uniaxial, **c** Nexus 5 MPU-6515, **d** S4 K330

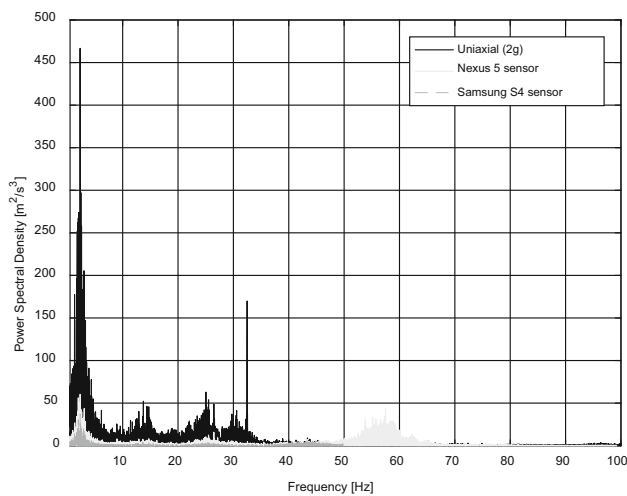


Fig. 7 Original acceleration spectra for test route 1

used to inspect video footage and time-stamped vehicle location coordinates.

Table 2 shows video screenshots corresponding to each peak and provides a description of each identified feature, highlighting that unique features are present at these locations. Peaks 0, 1, 2 and 3 were caused by speed bumps or road humps, while Peaks 4 and 7 were caused by manhole covers. Peak 6 was caused by a joint between old and new pavement surfaces. Peak 5 was caused by pavement repair strip for services crossing the road and is not detected by the Samsung S4 smartphone. Being able to identify these features by peak, location and timestamp allows significant features to be distinguished from others. It is noteworthy that of all these peak locations, Peak 5 gives the lowest peak response but identifies the only significant feature potentially requiring action, highlighting that acceleration peak magnitudes may not be reliable as the only discriminating criterion in urban areas.

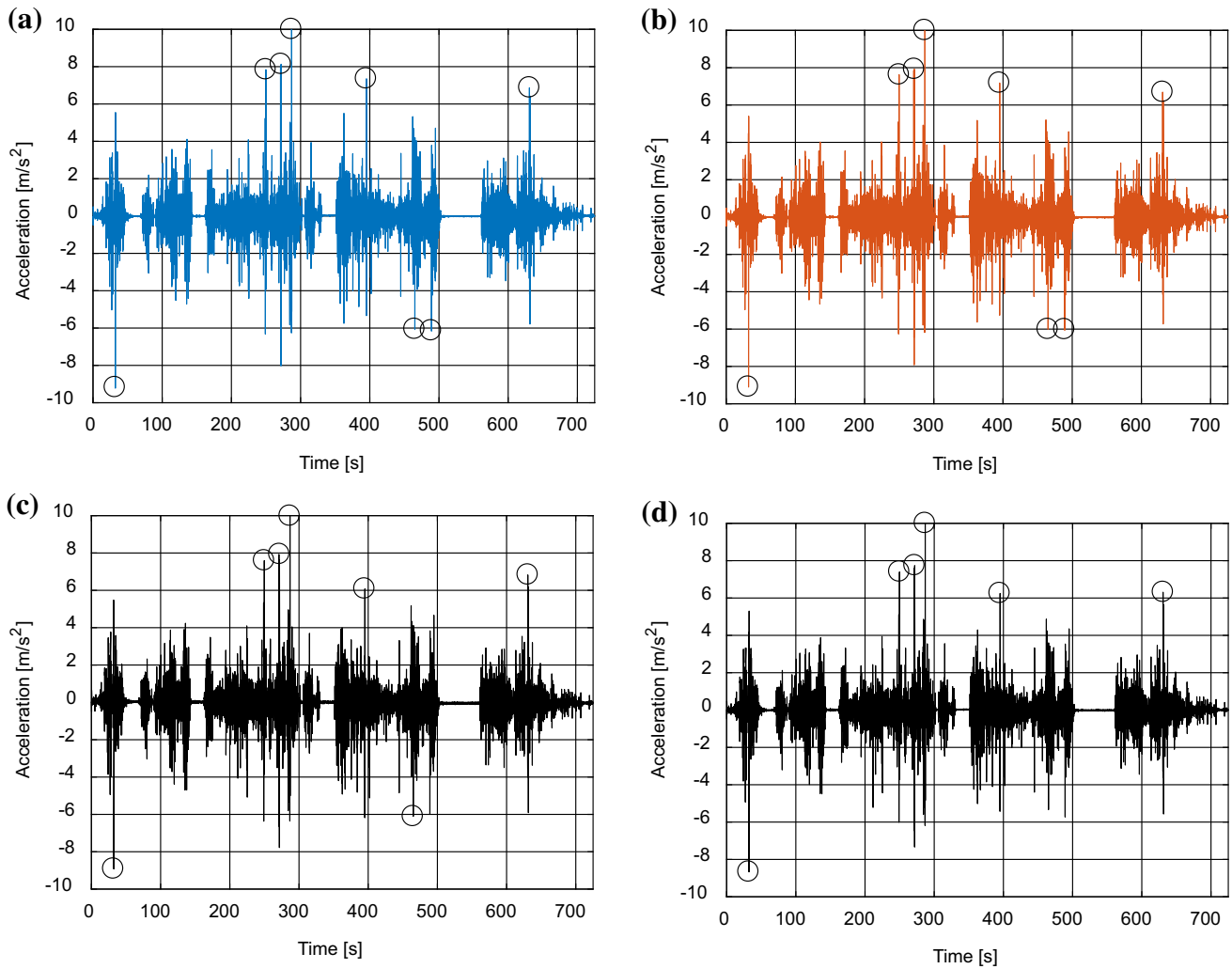


Fig. 8 Processed acceleration measurements for test route 1 **a** 5 g uniaxial, **b** 2 g uniaxial, **c** Nexus 5 MPU-6515, **d** S4 K330

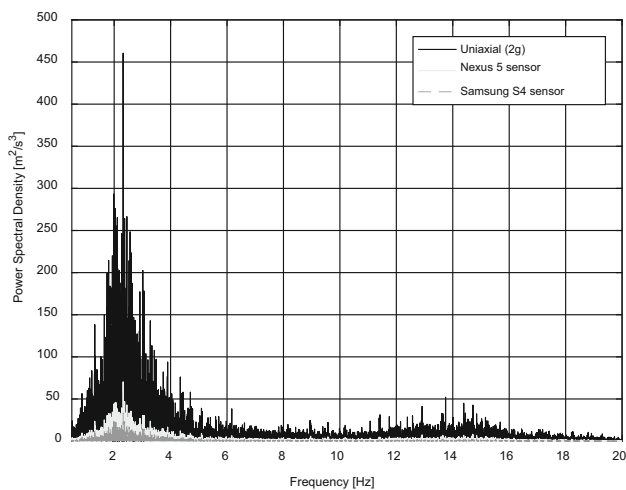


Fig. 9 Processed acceleration spectra for test route 1

3.1.2 Bridge expansion joints

Acceleration responses of the wired 2 g uniaxial accelerometer and the Nexus 5 accelerometer for test route 2 are shown in Fig. 11 for crossings of a two-span skew bridge. Each individual span is approximately 15.95 m, while the total cumulative span is 32.9 m over the M1 motorway on Dunmurry Lane, south of Belfast city. This bridge is of prestressed concrete beam and slab construction and was completed in 1965. The measured vehicle response was extracted based on the recorded position of the vehicle (Sect. 3.2) and inspection of video footage for test route 2. Similar responses can be observed for three repeated crossings—differences between measurements were primarily caused by variation in vehicle speed between crossings. Both accelerometers display three

Table 1 Times and magnitudes (in m/s^2) of peaks exceeding $\pm 6 \text{ m/s}^2$ on test route 1

	Peak 0	Peak 1	Peak 2	Peak 3	Peak 4	Peak 5	Peak 6	Peak 7
Time from start (s)	32	250	272	287	395	465	489	631
Real time (hh:mm:ss)	15:52:49	15:56:27	15:56:49	15:57:04	15:58:52	16:00:02	16:00:26	16:02:48
Accelerometer								
5 g uniaxial	−9.18	7.84	8.13	10.8	7.353	−6.06	−6.14	6.87
2 g uniaxial	−9.1	7.62	7.92	10.49	7.18	−6.01	−6.02	6.69
Nexus 5 MPU-6515	−8.92	7.59	7.93	9.98	6.08	−6.11	−	6.83
S4 K330	−8.67	7.40	7.74	10.19	6.25	−	−	6.31

periodic low-frequency disturbances. On inspection of video footage (Fig. 10), it can be confirmed that these correspond to the three expansion joints on the bridge, indicated by vertical dashed lines in Fig. 11. This shows that the drive-by monitoring system, at a minimum, can identify the vehicle's entry and exit to the bridge, and has potential to monitor deterioration of the expansion joint covering and/or the joint itself through analysis of the vehicle's dynamic response.

3.1.3 Bridge frequency identification

Siringoringo and Fujino [14, 15] note that expansion joints excite vehicle bounce and pitch motions and their dominance in the vehicle dynamic response can hide the bridge response. Therefore, it is recommended that this part of the signal should not be considered if bridge dynamic parameters are of interest. This introduces a further complication related to the length of the VBI signal obtained on a short span bridge crossing—any reduction in signal length can also reduce identification accuracy and make bridge frequency identification a very difficult task. For example, from Fig. 11 it can be seen that if the vehicle response excited by each expansion joint is removed, less than 2 s of measurement data would remain. To investigate whether the bridge frequency can be identified, the vehicle's acceleration response is processed using a fast Fourier transform (FFT). It should be noted that the bridge was not instrumented and its dynamic properties were not known a priori; therefore, vehicle dynamic responses from before (pre), during and after (post) the bridge crossing are compared for this reason. Equal data lengths are extracted for consistency. The resulting spectra for the wired 2 g accelerometer and the Nexus 5 accelerometer are shown in Fig. 12, comparing well despite the magnitude difference; the on-bridge data here correspond to Fig. 11a. Comparing the pre-bridge against on-bridge spectra, there are no clear peaks that can be distinguished as bridge frequency peaks. An overall increase in magnitude is observed, which was expected due to the excitation by expansion joints. A

unique peak does occur at 5.3 Hz for the Nexus 5 in the on-bridge response which is close to the frequency expected for a bridge of this form and span (~ 6 Hz). However, it is also found to occur in pre-bridge responses for other cases (not shown here) thus cannot be attributed to the bridge. Inspecting the post-bridge response, it is notable that vehicle-related frequency peaks around 14 Hz reappear that were not excited during the bridge crossing. A number of peaks from 7 to 12 Hz also occur for both the on- and post-bridge responses, respectively, potentially bridge related but most likely these indicate some particular vehicle mode(s) of vibration being excited only during the crossing.

A number of factors affect identification of the bridge frequency here, including the vehicle excitation by the expansion joint [14], short signal length and the relatively low mass of the vehicle which does not excite significant bridge vibration. Yang et al. [25] have proposed applying some filtering techniques to remove the vehicle frequency from the vehicle's acceleration spectra thus improving the visibility of the bridge frequency, provided the vehicle frequencies are known, e.g. from modal testing. Although clear bridge frequency identification is not achieved here, it is worth noting the shift in the apparent vehicle body bounce frequency from the value of 2.3 Hz observed in test 1—on bridge it increases to 2.7 Hz, while post-bridge it decreases to around 2 Hz. This could be caused by vehicle speed variation, but also could be due to coupling vibration with the bridge which would cause the apparent frequency of the vehicle to increase.

3.2 GNSS tracking measurements

Figure 14 shows the vehicle location coordinates logged and time-stamped during test route 1 by the Leica GS14 smart antenna. Peaks identified from the acceleration time histories which coincided with logged coordinates are indicated by numbered icons, highlighting that where video or imagery is unavailable in practice, the location of specific points of interest can be identified via GNSS.

Table 2 Description of identified pavement features for peaks exceeding $\pm 6 \text{ m/s}^2$ on test route 1









Peak	Video Screenshot	Description of Identified feature	Detected by smartphone
0		Speed bump	Yes
1		Flat top road hump	Yes
2		Flat top road hump	Yes
3		Flat top road hump	Yes
4		Service manhole	Yes
5		Pavement repair strip	Yes (Nexus 5 only)
6		Pavement joint	No
7		Pavement patch repair and service manholes	Yes



Fig. 10 Bridge expansion joints at crossing over M1 motorway on Dunmurry Lane on test route 2; **a** west entrance, **b** centre, **c** east entrance

These coordinates were logged manually as static points; thus, accuracy varied due to the movement of the vehicle; it can be seen that coordinates for peak 1 were thus not obtained. The coordinate quality ranged from 0.01 m in relatively open areas to 8 m in wooded areas. The largest causes of error were trees or wooded areas lining the road which obstructed clear open sky for the antenna.

The vehicle position coordinates logged by the Leica GS14 during test route 2 are shown in Fig. 15, where icons with black dots indicate two separate bridge crossings. The coordinate quality ranged 0.01–5.7 m, averaging at 0.4 m. A gap in recorded coordinates can be seen at the bottom left of this figure; this was caused by a temporary crash of the CS15 controller operating system. This can be overcome by automatically logging raw data to the GS14's internal memory, rather than manual operation as in this test. Overall, similar issues affecting accuracy were experienced as for route 1. In particular, at the M1 motorway bridge crossing (see Fig. 15 inset), overhanging trees restricted recording of location at the western entrance to the bridge (Fig. 13). In addition to raw data logging, this problem can be alleviated for GNSS systems by carrying out testing in winter rather than summer, when trees have shed their foliage. Other possible solutions include inertial navigation systems (INS), which incorporate accelerometers, gyroscopes, magnetometers and GNSS receivers, but an equivalent system for accurate vehicle tracking can be relatively expensive.

Figure 16 illustrates the vehicle position recorded by GPSEssentials during the second half test route 2, covering the gap in the Leica GS14 record. The rapid update of position and accuracy in the region of the M1 bridge crossing is particularly of note—for this application, its robustness has surpassed the Leica system. Overall it was observed that the smartphone accuracy was sufficient to identify when the vehicle was on the bridge. In terms of post-processing and visualising coordinates, GPSEssentials was very straightforward due to the output of a.kml format file; the Leica system required more user post-processing time to achieve the same output.

3.2.1 Comparison of tested GNSS systems

The Leica GS14 is designed for high precision surveying applications which require positioning errors <0.01 m, primarily static measurements. However, this level of accuracy requires information to be received via both L1 (1575.42 MHz) and L2 (1227.60 MHz) frequencies, which can result in poor robustness for moving measurements in urban or tree-lined routes. The system is affected by foliage and if signals are lost or satellite visibility is low, no location can be recorded, despite its use of the mobile network to provide RTK corrections [21]. This is illustrated in Figs. 15 and 16 which show coordinates recorded by the GS14 compared to the smartphone for the second half of route 2; the loss of satellite lock due to foliage prevented some coordinates being recorded. However, where such problems did not occur, position errors were less than 0.05 m. All Leica GS14 rover data were post-processed in Leica Geo Office against the QUB1 continually operating reference station (CORS), located at Queen's University Belfast, UK.

In contrast, the smartphone logged coordinates every second without any dropouts, due to its use of the L1 frequency only and assisted GPS via the mobile network [23]. In this investigation, the smartphone positioning error was approximately 2 m at best, and 20 m at worst; it is not possible to reach the accuracy of the GS14 with this technology at present. The advantages of utilising a smartphone to track geographical position are its robustness and its relative ease of use. However, as can be seen in Fig. 16 below, this level of accuracy is sufficient to identify the vehicle as being on the road and approximately when it crosses a bridge, although an exact lane position may not be confirmed. It is not affected by trees or foliage, although the smartphone's position inside the vehicle rather than external, as per the Leica system, can increase positioning errors. It is recommended that where possible, an antenna external to the vehicle would reduce the interference of the vehicle body with GNSS signals received by the smartphone thus improving the accuracy and reliability of the

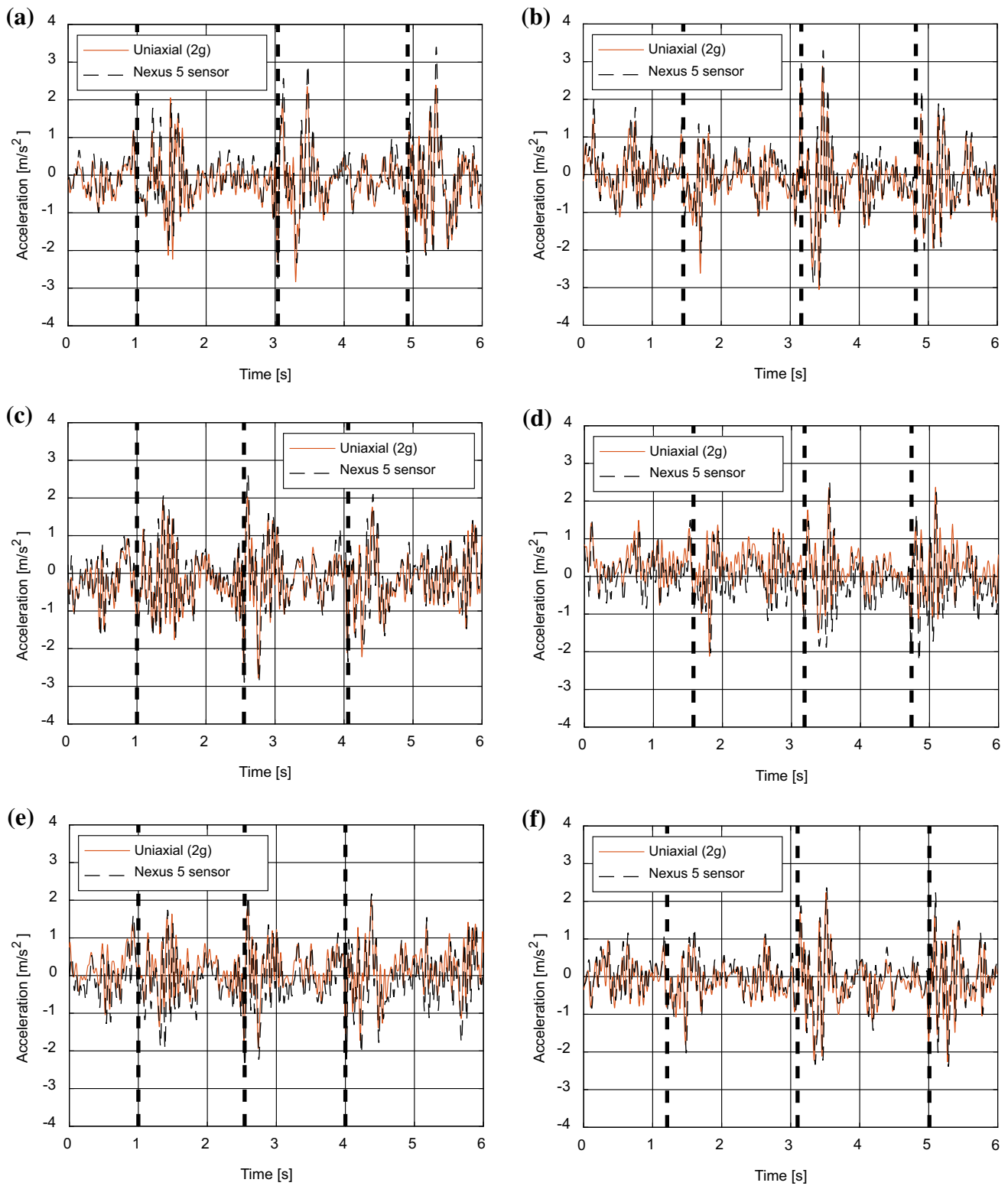


Fig. 11 Vehicle acceleration measurements from bridge crossing over M1 motorway **a** East crossing 1, **b** West crossing 1, **c** East crossing 2, **d** West crossing 2, **e** East crossing 3, **f** West crossing 3

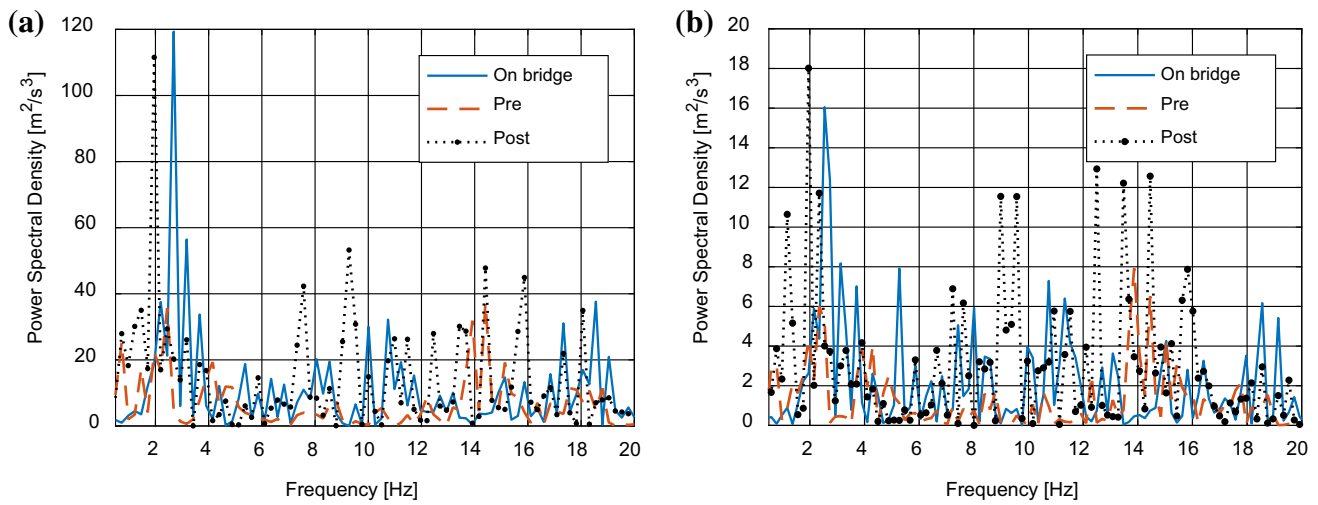


Fig. 12 Acceleration spectra for vehicle on bridge **a** uniaxial 2 g accelerometer, **b** Nexus 5 accelerometer



Fig. 13 West entrance to bridge crossing over M1 motorway on Dunmurry Lane on test route 2

recorded coordinates. Overall, it can be concluded that the level of accuracy provided by the smartphone is sufficient for most drive-by applications while from a cost perspective, it holds a huge advantage over the dedicated GNSS receiver.

4 System cost comparison

Table 3 presents an overall comparison of each sensor system tested. Comparing the smartphone sensors versus the wired accelerometers and Leica GS14 smart antenna in terms of cost is straightforward; the wired accelerometers and DAQ system cost in the region of €8000 in total, while the Leica GS14 smart antenna system can retail from €18,000 to €28,000, giving an overall system cost of at least €26,000. The equivalent cost of a smartphone is a

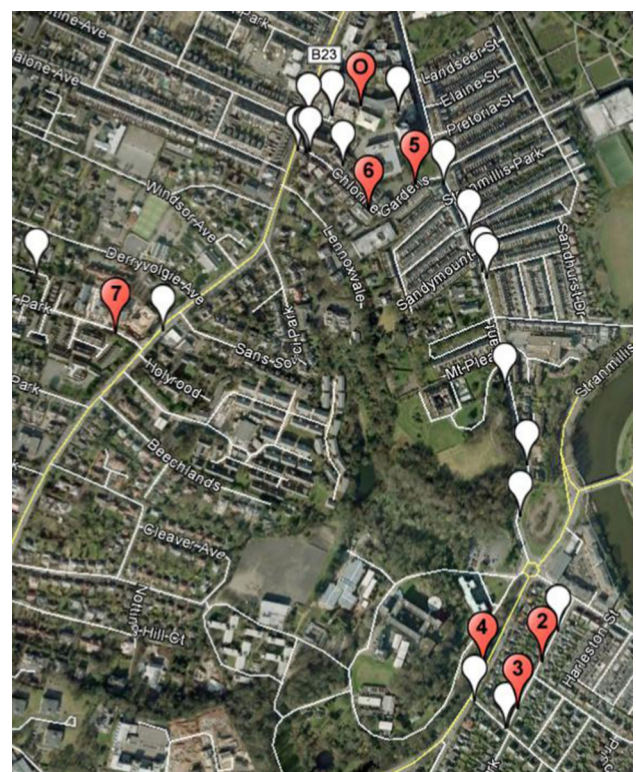


Fig. 14 Vehicle position coordinates logged using Leica GS14 for test route 1

factor of 100 less than this, giving a clear advantage to smartphone devices in terms of cost savings; 100 vehicles in a fleet could easily be used as monitoring vehicles using smartphone sensors for the same instrumentation cost as one specialised instrumented vehicle.

Fig. 15 Vehicle position coordinates logged using Leica GS14 on test route 2 **a** overview, **b** on bridge



Fig. 16 Vehicle position coordinates logged using GPSEssentials smartphone application on test route 2 **a** overview, **b** on bridge

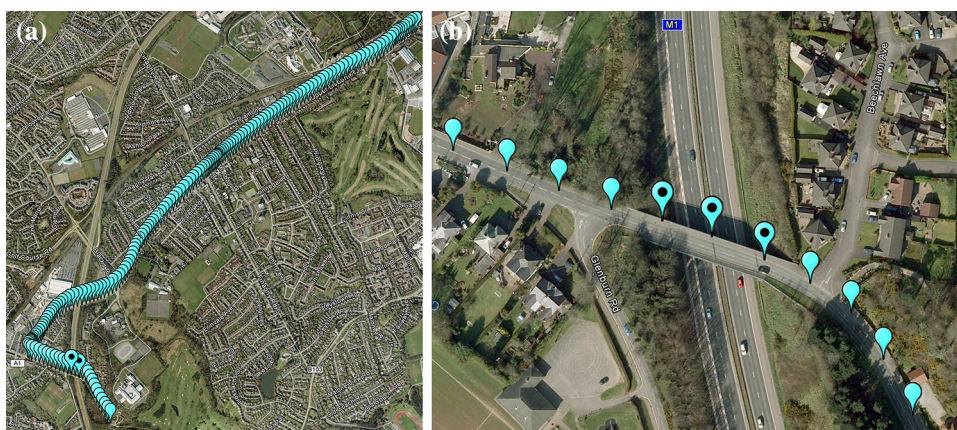


Table 3 Comparison of drive-by data acquisition systems

Equipment type	Approximate cost	Relative ease of use	Applicability	Accuracy
Leica GS14 GNSS Smart Rover	€18,000–€26,000	Low	Specialist vehicle	High (but requires open sky)
2G uniaxial accelerometer + DAQ system	€8000	Low–medium	Specialist vehicle	High
Smartphone GNSS	€250	High	Widespread	Medium–high
Smartphone accelerometer		High	Widespread	Medium

5 Conclusions

This paper has presented an investigation into the implementation of a drive-by monitoring system incorporating smartphone technology, comparing smartphone sensor performance with wired accelerometers, DAQ system and a Leica GS14 smart antenna. A comparison in terms of cost is straightforward; the smartphone system cost is a factor of 100 less than the alternative specialist equipment, giving a clear advantage to smartphone devices in terms of cost savings and potential implementation of drive-by methods via instrumented vehicle fleets. However, further study on

fleet implementation is required as there are qualitative limitations to application of existing drive-by monitoring algorithms to crowdsourced acceleration data, e.g. consistent sampling rates, sensor type, position and orientation will influence application of algorithms to raw data.

The smartphone applications tested were convenient, easy to use and involved less effort for post-processing vehicle location coordinates, reducing the need for any specialist training in identifying the vehicle's position in a road network. Furthermore, the general level of accuracy illustrated by the smartphone acceleration measurements based on the tested sampling frequency, range and output

acceleration spectra indicates that it should be feasible to use these signals for drive-by, or general, structural health monitoring approaches. Further analysis of the acceleration signals and corresponding spectra magnitude is required to establish their suitability for bridge dynamic parameter and damage detection algorithms. This will include further field testing, including instrumentation of the tested bridge.

Acknowledgements The authors wish to express their gratitude for the technical support received by Mr. Kenny McDonald, Mr. Jamie Laing, and Mr. Conor Graham of Queen’s University Belfast during the course of this investigation.

Open Access This article is distributed under the terms of the Creative Commons Attribution 4.0 International License (<http://creativecommons.org/licenses/by/4.0/>), which permits unrestricted use, distribution, and reproduction in any medium, provided you give appropriate credit to the original author(s) and the source, provide a link to the Creative Commons license, and indicate if changes were made.

References

- Fujino Y, Siringoringo DM (2011) Bridge monitoring in Japan: the needs and strategies. *Struct Infrastruct Eng Maint Manag Life Cycle Des Perform* 7(7–8):597–611
- Chupanit P, Phromsorn C (2012) The importance of bridge health monitoring. *Int Sci Index* 6:135–138
- Rytter A (1993) Vibration based inspection of civil engineering structures. Aalborg University, Denmark
- Carden EP, Fanning P (2004) Vibration based condition monitoring: a review. *Struct Health Monit* 3:355–377
- Sayers MW, Karamihas SM (1998) The little book of profiling. University of Michigan Transportation Research Institute, UMTRI-96-19
- Lin CW, Yang YB (2005) Use of a passing vehicle to scan the fundamental bridge frequencies: an experimental verification. *Eng Struct* 27:1865–1878
- Malekjafarian A, McGetrick PJ, O'Brien EJ (2015) A review of indirect bridge monitoring using passing vehicles. In: *Shock and vibration*, vol 2015. Article ID 286139. doi:10.1155/2015/286139
- McGetrick PJ, Kim CW, González A, O'Brien EJ (2013) Dynamic axle force and road profile identification using a moving vehicle. *Int J Archit Eng Constr* 2(1):1–16
- Yang YB, Lin CW, Yau JD (2004) Extracting bridge frequencies from the dynamic response of a passing vehicle. *J Sound Vib* 272:471–493
- Yang YB, Chang KC (2009) Extracting the bridge frequencies indirectly from a passing vehicle: Parametric study. *Eng Struct* 31:2448–2459
- Gonzalez A, O'Brien EJ, McGetrick PJ (2012) Identification of damping in a bridge using a moving instrumented vehicle. *J Sound Vib* 331:4115–4131
- Oshima Y, Yamamoto K, Sugiura K (2014) Damage assessment of a bridge based on mode shapes estimated by responses of passing vehicles. *Smart Struct Syst* 13:731–753
- Zhang Y, Lie ST, Xiang ZH (2013) Damage detection method based on operating deflection shape curvature extracted from dynamic response of a passing vehicle. *Mech Syst Signal Process* 35:238–254
- Siringoringo DM, Fujino Y (2012) Estimating bridge fundamental frequency from vibration response of instrumented passing vehicle: analytical and experimental study. *Adv Struct Eng* 15:417–433
- Fujino Y, Kitagawa K, Furukawa T, Ishii H (2005) Development of vehicle intelligent monitoring system (VIMS). In: *Proceedings of SPIE 5765, smart structures and materials 2005: sensors and smart structures technologies for civil, mechanical, and aerospace systems*
- Miyamoto A, Yabe A (2012) Development of practical health monitoring system for short- and medium-span bridges based on vibration responses of city bus. *J Civ Struct Health Monit* 2:47–63
- McGetrick PJ, Kim CW, González A, O'Brien EJ (2015) Experimental validation of a drive-by monitoring system for bridges. *Struct Health Monit* 14(4):317–331
- Stedman II, C, DeMarco A (2007) Automated GPS mapping of road roughness. Worcester Polytechnic Institute
- Poncela A, de Diego V, Lorenzana A, de Sebastian J (2011) Automatic portable system for fault detection in the pavement of roads using wireless sensors and GPS. In: *Proceedings of the 5th international conference on structural health monitoring of intelligent infrastructure (SHMII-5)*, 11–15 December 2011, Cancún, Mexico
- Carrera F, Guerin S, Thorp BJ (2013) By the people, for the people: the crowdsourcing of “Streetbump”, an automatic pothole mapping app. In: *International archives of the photogrammetry, remote sensing and spatial information sciences*, vol XL-4/W1, 29th Urban data management symposium (UDMS 2013), 29–31 May, 2013, London, UK
- Takac F, Lienhart W (2008) SmartRTK: a novel method of processing standardised RTCM network RTK information for high precision positioning. In: *Proceedings of ENC GNSS 2008*, 22–25 April 2008, Toulouse, France
- Schollmeyer M (2015) GPS essentials manual. <http://www.gpsessentials.com>
- Zandbergen PA, Barbeau SJ (2011) Positional accuracy of assisted GPS data from high-sensitivity gps-enabled mobile phones. *J Navig* 64(3):381–399. doi:10.1017/S0373463311000051
- Gikas V, Perakis H (2016) Rigorous performance evaluation of smartphone GNSS/IMU sensors for ITS applications. *Sensors* 16:1240. doi:10.3390/s16081240
- Yang YB, Chang KC, Li YC (2013) Filtering techniques for extracting bridge frequencies from a test vehicle moving over the bridge. *Eng Struct* 48:353–362